

Interference effect of doorway states in a radiative capture reaction

Yu-Kun Ho*

*Centre of Theoretical Physics, China Centre of Advanced Science and Technology (World Laboratory), Beijing, China
and Nuclear Science Department, Fudan University, Shanghai 200433, China*

Wei-Juan Zhao

Nuclear Science Department, Fudan University, Shanghai, China

(Received 12 June 1992)

This work investigates the interference in radiative nucleon capture reactions between the giant resonances and the doorway configurations mixed in compound nucleus levels. A unified formalism has been established by which it is possible to study the interference among the four parts in the capture amplitude: the potential capture, valence capture, semidirect capture, and fine resonance capture stemming from doorway configurations. The $^{12}\text{C}(p, \gamma_0)$ data in the excitation energy region of 10–30 MeV in ^{13}N were analyzed by means of this formalism with an emphasis on investigating the dips and peaks superimposed on the pigmy resonance. These structures are interpreted as destructive or constructive interferences in doorway configurations. Parameters for both the giant resonances and fine levels were extracted by fitting the measured data. We extend the study to discuss the potential of observing similar interferences in the reactions $^{12}\text{C}(n, \gamma_0)$ and $^{12}\text{C}(p, \gamma_n)^{13}\text{N}^*$, leading to excited states of the final nucleus.

PACS number(s): 25.40.Lw, 24.10.−i, 27.20.+n

I. INTRODUCTION

In previous papers [1,2], the interference effect in the channel radiative capture reaction has been investigated. Those studies show that the neutron capture data in ^{12}C at a neutron energy less than 30 keV can be well understood in terms of the channel capture mechanism. Of most interest, the destructive interference between potential capture and valence capture is indicated to be crucial in understanding the very small thermal neutron capture cross sections in ^{12}C and its neighbor nuclides. Both potential capture and valence capture stem from the one-quasiparticle configurations (the entrance channel configurations) in the capture states. The potential capture comes from the shape elastic-scattering wave, and the valence capture [3] arises from the compound (resonance) elastic-scattering wave.

The next kind of simple configuration, which is important to the radiative capture reactions, consists of the doorway states [4] (the three-quasiparticle configurations), such as the giant dipole resonances for $E1$ transitions. Similar to the entrance channel configurations, the doorway states can be reached by two approaches different on the reaction time scale in nucleon-induced reactions. The semidirect capture [5] is a process where the doorway states are reached in a prompt way, which shows giant resonance behavior with widths on the order of a few MeV. As the slowest extreme, the part of the doorway strength which is mixed

into the complex fine levels can be reached by the compound nucleus process. Those two parts of the radiative strength are expected to interfere, and the question is where to find clear evidence of this interference effect.

The best way to identify the interference is to look for dips caused by destructive interference between discrete narrow levels and giant resonances with evidence that both the giant resonance strength and the level radiative strength arise from the doorway states. Nucleon capture in light magic nuclei, such as ^{12}C and ^{16}O , provide good chances to find this effect. This is because the level densities in those nuclei are fairly low compared with those of the medium and heavy nuclei. The discrete levels are extended to the energy range of giant resonances, and so it is possible to observe distinct fine structure on giant resonances. In addition, experimental measurements [6,7] have confirmed that a considerable fraction of the dipole strength goes down to a lower energy region to form so-called pigmy resonances for those nuclei with a closed shell plus one or two nucleons. This behavior would make the interference clearer. In addition, the weak coupling between the valence nucleon and the light closed-shell nucleus makes the configurations involved relatively simple and affords easier analysis for the capture amplitude.

Section II presents a unified formalism to study radiative capture reaction cross sections. With this formalism, it is possible to investigate the interferences among the four parts of the capture amplitude: namely, potential capture, valence capture, semidirect capture, and narrow resonance capture due to doorway configurations. In Sec. III, the $^{12}\text{C}(p, \gamma_0)$ data are analyzed in terms of the above formalism. Emphasis will be put on the narrow levels with spin-parity of $\frac{3}{2}^+$ interfering with the broad dipole resonances of $J^\pi = \frac{3}{2}^+$ in a way that attempts to

*Mailing address: Nuclear Science Department, Fudan University, Shanghai 200433, China.

identify the interference in the doorway states and extract relevant parameters for both the giant resonances and narrow levels. In addition, the mirror nuclei ^{13}C and ^{13}N are well known to have corresponding levels, and the two reactions $^{12}\text{C}(n, \gamma_0)$ and $^{12}\text{C}(p, \gamma_0)$ have their major characteristic in common. A pigmy resonance also has been observed in the reaction $^{12}\text{C}(n, \gamma_0)$. In addition, since the first excited state (2.36 MeV, $\frac{1}{2}^+$) and the third one (3.547 MeV, $\frac{5}{2}^-$) in ^{13}N are of prominent single-particle characteristics, it is expected that the reactions $^{12}\text{C}(p, \gamma_1)$ and $^{12}\text{C}(p, \gamma_3)$ would exhibit pigmy resonances. Therefore, it is of interest to extend the present study to see the potential of finding a similar interference structure in those radiative capture reactions. Section IV is a brief summary.

II. FORMALISM

The radiative nucleon capture cross section from an initial capture state Ψ_i to a final state Ψ_f is, in the case of electric dipole transition,

$$\sigma_{n\gamma, f} = \frac{16\pi}{9} \frac{m^2}{\hbar^2} \frac{k_\gamma^3}{k} |\langle \Psi_f | e\mathcal{D} | \Psi_i \rangle|^2, \quad (1)$$

where m is the reduced mass, and k_γ and k are the wave numbers of the outgoing photon and the incoming nucleon, respectively. $e\mathcal{D}$ is the total electric dipole transition operator, which can be elaborated as

$$\mathcal{D} = \mathcal{D}_c + d, \quad (2)$$

where \mathcal{D}_c and d act on the target and valence nucleon, respectively.

In the present case, Ψ_i includes the entrance channel (one-quasiparticle) configurations $\psi_i^{(1)}$, and the doorway states (three-quasiparticle configurations) important to the capture reaction $\psi_i^{(3)}$. The wave function should be normalized to meet the initial condition of a standard plane incoming wave $e^{ikz} \kappa_{m_s}$, where m_s denotes the spin projection. Then, one has

$$\Psi_i^{(1)} = \sum_i i \frac{\sqrt{(2l+1)\pi}}{kr} \mathcal{U}_{lj}^J(r) \mathcal{C}_{l0m_s}^{jm_s} \mathcal{C}_{jm_s, l m_s}^{Jm} \phi_{lj}^{Jm}, \quad (3)$$

where

$$\mathcal{U}_{lj}^J(r) = \frac{-2i}{1 - i\mathcal{H}_{lj}^J} \mathcal{U}_{lj}^J(r), \quad (4)$$

and

$$\mathcal{U}_{lj}^J(r) = \text{Re} \langle \mathcal{U}_{lj}^J(r) \rangle + \frac{1}{2} \sum_{\lambda(J)} \frac{\Gamma_{\lambda c}}{E_\lambda - E - (i/2)\Gamma_\lambda} \mathcal{N}_{lj}(r) \quad (5)$$

is the scattering radial wave function,

$$\mathcal{N}_{lj}(r) = \frac{\text{Im} \langle \mathcal{U}_{lj}^J(r) \rangle}{\text{Im} \langle \mathcal{H}_{lj}^J \rangle}. \quad (6)$$

Re and Im designate real and imaginary parts, $\langle \mathcal{H}_{lj}^J \rangle$ is the optical-model reactance matrix element, $\langle \mathcal{U}_{lj}^J(r) \rangle$ is

the optical-model scattering wave function, the \mathcal{C} 's are Clebsch-Gordan coefficients, and the quantity

$$\phi_{lj}^{JM} = [\mathcal{Y}_{lj} \times \Phi_{0l}]^{JM} \quad (7)$$

is the channel wave function consisting of the intrinsic ground-state wave function of the target nucleus, Φ_{0l} , coupled to the nucleon angular momentum wave function \mathcal{Y}_{lj} to give total spin J and projection M . In Eq. (5), λ refers to a nearby fine level. The reader is referred to the original article [1] for the nomenclature.

The two terms in Eq. (5) are the potential scattering wave and resonance compound nucleus scattering wave, corresponding to the potential capture and valence capture, respectively.

The single-particle configuration in the final state Ψ_f , which is able to contribute to the transition matrix element in Eq. (1), is

$$\psi_f^{(1)} = \sqrt{S_f} \frac{\mathcal{U}_{l_f j_f}(r)}{r} \phi_{l_f j_f}^{J_f M_f}, \quad (8)$$

where s_f denotes the (d, p) spectroscopic factor associated with the final state f .

Similar to the entrance channel configurations, there are also two parts for the doorway states. One appears as giant resonances. The other appears in fine resonances. The former can be reached in a prompt way in capture reaction, the semidirect capture, and may be written as [8]

$$\psi_i^{(3s)} = \sum_g \frac{b_g}{E - E_g + (i/2)\Gamma_g} \times \langle \psi_{-1, f}^{(3)} | \mathcal{V}' | \psi_i^{(1s)} \rangle \psi_{-1, f}^{(3)}, \quad (9)$$

where E_g , Γ_g , and b_g are the parameters designating the energy centroid, width, and strength fraction of g th giant resonance, respectively. In Eq. (9), we introduce the sum over index g to phenomenologically model the possible split of the giant dipole resonance (GDR) due to nuclear deformation or appearance of a pigmy resonance. $\psi_i^{(1s)}$ represents the potential scattering part in Eq. (3),

$$\mathcal{V}' = \left[\frac{3}{4\pi} \right]^{1/2} \mathcal{K}'(r) \mathcal{Y}_{1\mu}^*(\theta, \phi) \omega_\mu \quad (10)$$

is the particle-phonon coupling potential, ω_μ is the μ component of the relative coordinate vector of the neutron center of mass to that of the proton ($\vec{\omega} = \vec{R}_n - \vec{R}_p$), $\mathcal{K}'(r)$ is the coupling form factor, $\psi_{-1, f}^{(3)}$ represents the core dipole excitation wave function with a valence nucleon remaining in the orbit of the final state f ,

$$\psi_{-1, f}^{(3)} = \frac{1}{r} \mathcal{U}_{l_f j_f}(r) [\mathcal{D}_c^\dagger \times (\mathcal{Y}_{l_f j_f} \times \Phi_{0l})^{J_f M_f}]^{JM}, \quad (11)$$

where

$$(\mathcal{D}_c^\dagger)_\mu = - \left[\frac{3}{4\pi} \right]^{1/2} \frac{NZ}{A} \omega_\mu \quad (12)$$

is the creation operator of the core dipole excitation.

The part of the doorway configurations mixed into the fine levels in the capture state is of the form

$$\begin{aligned} \psi_i^{(3R)} = & i \frac{\sqrt{(2l+1)\pi}}{k} (-2i) \mathcal{O}_{l0m_s}^{j m_s} \mathcal{O}_{j m_s l m_l}^{J M} \\ & \times \frac{1}{2} \sum_{\lambda} \frac{\Gamma_{\lambda c}^{1/2}}{E_{\lambda} - E - (i/2)\Gamma_{\lambda}} a_{\lambda}^{(3)} \psi_{-1,f}^{(3)}, \end{aligned} \quad (13)$$

where $a_{\lambda}^{(3)}$ designates the configuration coefficient of the doorway state $\psi_{-1,f}^{(3)}$ in the level λ .

Inserting Eqs. (3), (9), and (13) into Eq. (1) for the initial state and Eq. (8) for the final state, performing the average over the initial state and sum over the final state, yields

$$\sigma_{n\gamma,f}^{(1,3)} = \frac{\pi}{k^2} \sum_{ijj'} \frac{2J+1}{2(2I+1)} \left| \left[\mathcal{T}_{ijj',f}^{(1)} + \mathcal{T}_{ijj',f}^{(3)} + \sum_{\lambda(J)} \frac{\gamma_{\lambda c}(\gamma_{\lambda\gamma f}^{(1)} + \gamma_{\lambda\gamma f}^{(3)})}{E_{\lambda} - E - (i/2)\Gamma_{\lambda}} \right] \right|^2, \quad (14)$$

where

$$\begin{aligned} \mathcal{T}_{ijj',f}^{(1)} = & \sqrt{(4/3)(k_{\gamma}^3/\hbar v)} \langle l_j J | D_I | l_{fj} J_f \rangle (2J_f + 1) S_f \\ & \times \bar{e} \int \langle \mathcal{U}_{ij}^{(1)}(r) \rangle r \mathcal{U}_{ijj',f}(r) dr \end{aligned} \quad (15)$$

is the potential (direct) capture amplitude, and

$$\begin{aligned} \mathcal{T}_{ijj',f}^{(3)} = & \sqrt{(4/3)(k_{\gamma}^3/\hbar v)} \langle l_j J | D_I | l_{fj} J_f \rangle (2J_f + 1) S_f \\ & \times e \int \langle \mathcal{U}_{ij}^{(3)}(r) \rangle r \mathcal{A}(r) \mathcal{U}_{ijj',f}(r) dr \end{aligned} \quad (16)$$

is the semidirect capture amplitude. In these equations, \bar{e} is the nucleon effective charge ($-Ze/A$ for neutron, Ze/A for proton). $\langle l_j J | D_I | l_{fj} J_f \rangle$ is the reduced matrix element of the angular-spin part. In Eq. (16),

$$\begin{aligned} \mathcal{A}(r) = & -\frac{ZN}{2A^2} \frac{\sigma_{-1}}{0.096 \langle r^2 \rangle (NZ/A)} \\ & \times \sum_g \frac{b_g}{E - E_g + (i/2)\Gamma_g} \\ & \times \left[V_{1f}(r) - iW_{14b} \frac{df(r)}{dr} \right] \end{aligned} \quad (17)$$

and

$$f(r) = \left[1 + \exp \left(\frac{r-R}{a} \right) \right]^{-1}. \quad (18)$$

In Eq. (17),

$$\frac{\sigma_{-1}}{0.096 \langle r^2 \rangle (NZ/A)} = 1 + \beta$$

and β specifies the contribution due to terms which do not commute with the dipole operator [5]. In Eq. (14), $\Gamma_{\lambda c} = |\gamma_{\lambda c}|^2$ is the level nucleon width,

$$\begin{aligned} \gamma_{\lambda\gamma f}^{(1)} = & \sqrt{(4/3)(k_{\gamma}^3/\hbar v)} \langle l_j J | D_I | l_{fj} J_f \rangle (2J_f + 1) S_f \\ & \times \frac{\bar{e}}{1 - i \langle \mathcal{U}_{ij}^{(1)} \rangle} \gamma_{\lambda c} \int \mathcal{N}_{ij}(r) r \mathcal{U}_{ijj',f}(r) dr \end{aligned} \quad (19)$$

is the level valence radiative amplitude, and $\Gamma_{\lambda\gamma f}^{(1)} = |\gamma_{\lambda\gamma f}^{(1)}|^2$ is the level valence radiative width,

$$\gamma_{\lambda\gamma f}^{(3)} = \sqrt{(32\pi/9)(k_{\gamma}^3/\hbar v)(1+\beta)s_f} \frac{NZ}{A} e a_{\lambda}^{(3)} \quad (20)$$

is the level radiative doorway amplitude, and $\Gamma_{\lambda\gamma f}^{(3)} = |\gamma_{\lambda\gamma f}^{(3)}|^2$ is the level radiative doorway width.

As clearly exhibited, Eq. (14) contains all the interference effects in nonstatistical capture reactions. The two terms $\mathcal{T}_{ijj',f}^{(1)}$ and $\gamma_{\lambda c} \gamma_{\lambda\gamma f}^{(1)}$ give rise to the interference in the channel capture [1]. The cross term between $\mathcal{T}_{ijj',f}^{(1)}$ and $\mathcal{T}_{ijj',f}^{(3)}$ is the well-known direct-semidirect interference. The interference in doorway states stems from the two amplitudes $\mathcal{T}_{ijj',f}^{(3)}$ and $\gamma_{\lambda c} \gamma_{\lambda\gamma f}^{(3)}$.

III. $^{12}\text{C}(p, \gamma_0)$ REACTION AND INTERFERENCE IN DOORWAY STATES

In this section, the data of the reaction $^{12}\text{C}(p, \gamma_0)$ in the excitation energy region in ^{13}N of 10–30 MeV will be examined, and model calculations based upon the above formalism will be made in a way that attempts to fit the measured data, extract parameters, and explore the interference effect concerned.

The measured capture cross sections [6,9–13] of the reaction $^{12}\text{C}(p, \gamma_0)$ are plotted in Fig. 1, exhibiting the fol-

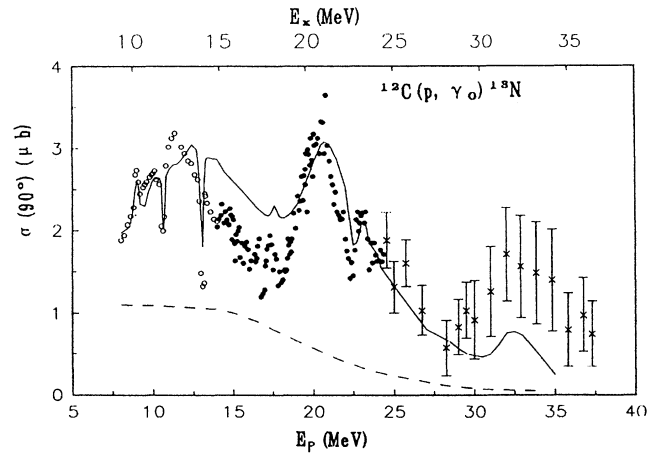


FIG. 1. Composite yield curve of capture γ ray in the reaction $^{12}\text{C}(p, \gamma_0)^{13}\text{N}$. The data are taken from Refs. [9–13]. The solid line is the calculated results based upon the formalism given by Eq. (14) with parameters shown in Tables I and II. The dashed line is the calculated potential capture cross sections.

lowing features: (1) two broad bumps centered at $E_x = 13$ and 21 MeV with widths of 7 and 4 MeV, respectively; (2) two strong destructive interference minima (dips) at $E_x = 11.74$ and 14.04 MeV; and (3) a number of peaks at $E_x = 10.25, 15.1, 18.15,$ and 23 MeV. The mean level space in the energy region is about $\bar{D} = 0.4$ MeV [6], while the mean level width is $\bar{\Gamma} = 0.25$ MeV. This means that the energy region with which we are concerned is still in the discrete-level range. In addition, most levels in this region do not have observable strength in the (p_0, γ_0) channel [6]. All those features make it possible to observe clear fine structure on the giant resonances.

Both the giant resonances appearing in Fig. 1 are of isospin $T_< = \frac{1}{2}$, and spin-parity $J^\pi = \frac{3}{2}^+$. The lower-energy one is often called the pigmy resonance although it is really too large to justify this name. The microscopic structure of those broad resonances so far is not completely understood [14,15]. Most of the strengths shown here are of $E1$ in character. Measurements of the polarized proton beam and angular distribution indicate that the total $E2$ capture cross sections are of the order of 0.2 μb and no resonance structure was observed [11–13].

There are four levels in the studied regions identified to have a spin-parity of $\frac{3}{2}^+$, and expected to interfere with the broad resonances. The two dips at $E_x = 11.74$ and 14.04 MeV are due to destructive interference, and the two peaks at $E_x = 18.15$ and 23 MeV are attributed to constructive interference. As will be indicated shortly, the valence widths for those levels calculated in terms of Eq. (19) are much less than the extracted total radiative widths (see Table II). Thus, most of the level radiative widths stem from the doorway configurations, and the observed dips afford unambiguous evidence for the interference in doorway states.

Using the formalism given in Eq. (14), the proton capture cross sections feeding the ground state in ^{13}N have been calculated in the energy region $E_x = 10\text{--}30$ MeV. The global optical-model potentials and parameters of Ref. [16] were used to calculate the nucleon transmission coefficients and the optical-model wave functions. The real part of the same potential is used to calculate the eigenvalues and eigenfunctions of the bound single-particle states. It should be stressed that the present calculations are not sensitive to the details of the optical potential. Only the real part of the global potential [16] was slightly adjusted to reproduce the measured nucleon binding energies. By fitting the measured data, the parameters for both the giant resonances (semidirect capture) and the fine levels have been extracted and given in Tables I and II, respectively. The calculated valence widths for the concerned levels are also presented in Table II. It can be seen that the valence mechanism is inadequate to account for the extracted level radiative widths. The calculated $^{12}\text{C}(p, \gamma_0)$ cross sections are shown in Fig. 1 as a solid line. The dashed line plotted in Fig. 1 represents the calculated results including only the $E1$ direct capture, which is also inadequate to reproduce the background of the measured cross sections.

The pigmy resonance was also found in the reaction $^{12}\text{C}(n, \gamma_0)$, although the data there [17–20] are sufficiently

TABLE I. Form factors for nucleon semidirect capture in ^{12}C . See Eq. (17) and the text for nomenclature. The nuclear radius and surface thickness in Eq. (18) were taken to be the same as the real part of the adopted optical potential.

		$^{12}\text{C}(p, \gamma_0)$	$^{12}\text{C}(n, \gamma_0)$
Pigmy resonance	E_g (MeV)	13.0	13.0
	Γ_g (MeV)	7.0	5.0
	$b\sigma_{-1}$ (b)	0.05	0.05
GDR	E_g (MeV)	21.0	21.0
	Γ_g (MeV)	4.0	2.5
	$b\sigma_{-1}$ (b)	0.017	0.017
Coupling parameters	V_1 (MeV)	65.0	65.0
	W_1 (MeV)	30.0	30.0
	b (fm)	0.55	0.55
	$\langle r^2 \rangle$ (fm ²)	14.0	14.0

poor that no fine structure is seen, so none appears. The related direct-semidirect model calculations along with the data are presented in Fig. 2, and the model parameters of semidirect capture form factors extracted from the fitting are listed in Table I. The mirror nuclides ^{13}C and ^{13}N are fairly similar in many aspects of nuclear properties, such as the corresponding low-lying level structure, electromagnetic transitions between the low-lying states, the positions and excitations of the $T_> = \frac{3}{2}$ states around $E_x = 15$ MeV, the pigmy resonances at $E_x = 13$ MeV, and GDR at $E_x = 21$ MeV. It is expected that there would be similar interference structure (dips and peaks) in the pigmy resonance and GDR region in $^{12}\text{C}(n, \gamma_0)$ as that of $^{12}\text{C}(p, \gamma_0)$. In fact, the early measured data of $^{13}\text{C}(\gamma, n)$ showed peaks at 11.0, 13.8, 16.5, and 17.8 MeV superimposed on the pigmy resonance and shoulder resonances at 20.8 and 30 MeV on GDR [21]. Also, a structure was found in the coefficients of the Legendre polynomial p_2 at $E_x = 20.5$ MeV, which was referred to as a secondary doorway state [22]. At the present stage, the primary task for experimental measurements in this reaction is to

TABLE II. Narrow levels concerned in ^{13}N , which have $J^\pi = \frac{3}{2}^+$ and observable strengths in the channel $(p_0\gamma_0)$. Γ_λ is the level total width. $\Gamma_{\lambda c}$ is the proton width. $\gamma_{\lambda\gamma f} = \gamma_{\lambda\gamma f}^{(1)} + \gamma_{\lambda\gamma f}^{(3)} = (\Gamma_{\lambda\gamma f})^{1/2} e^{i\theta}$ is the total radiative amplitude feeding the ground state. $\Gamma_{\lambda\gamma f}^{(1)}$ is the valence width. D represents destructive and C represents constructive.

E_λ (MeV)	11.74	14.04	18.15	23.0
J^π	$\frac{3}{2}^+$	$\frac{3}{2}^+$	$\frac{3}{2}^+$	$\frac{3}{2}^+$
Γ_λ (keV)	250	180	322	900
$\Gamma_{\lambda c}$ (keV)	70	126	30	70
$\gamma_{\lambda\gamma f}$: $\Gamma_{\lambda\gamma f}$ (eV)	4.2	3.7	3.2	5.5
θ (deg)	90	180	0	90
$\Gamma_{\lambda\gamma f}^{(1)}$ (eV)	0.09	0.08	0.058	0.014
Interference	D	D	C	C

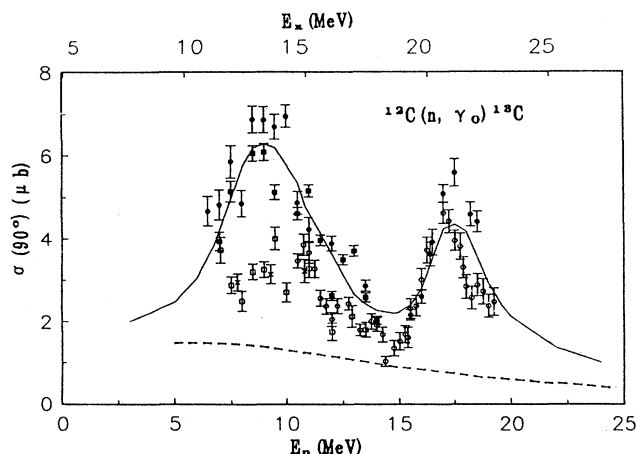


FIG. 2. The same as in Fig. 1 but for $^{12}\text{C}(n, \gamma_0)^{13}\text{C}$. The data are taken from Refs. [17–20].

identify the source of the discrepancy from different laboratories [17–20] for the $^{12}\text{C}(n, \gamma_0)$ data in the pigmy resonance region centered around 13 MeV.

A few additional comments may be made concerning the reactions $^{12}\text{C}(p, \gamma_n)$, which lead to excited states of the final nucleus. The first and third excited states in ^{13}N (2.345 MeV, $\frac{1}{2}^+$ and 3.547 MeV, $\frac{5}{2}^+$) have been found being of large (d, p) spectroscopic factors [6]. It is most likely that the reactions $^{12}\text{C}(p, \gamma_1)$ and $^{12}\text{C}(p, \gamma_3)$ would present pigmy resonances and interference structure. The early measured data [10, 22, 23] seem to show a GDR located at $E_x = 26$ MeV and a pigmy resonance at $E_x = 21$ MeV in the $^{12}\text{C}(p, \gamma_{23})$ cross sections. Most of the strength comes from the $f_{7/2} - d_{5/2}$ transitions [24]. In addition, the $^{16}\text{O}(p, \gamma_0)$ data [7] also shed some light on the conjecture on $^{12}\text{C}(p, \gamma_3)$. This reaction shows a GDR lying at $E_x = 22$ MeV and a pigmy resonance at $E_x = 17.5$ MeV, stemming mainly from $\frac{7}{2}^- - \frac{5}{2}^+$ transitions. The ground state of ^{17}O possesses a big $d_{5/2}$ spectroscopic factor. We note the advent of new tagged beam techniques [25–27] has made it possible to get precision measurements of those radiative capture reactions leading to ex-

cited states. Obviously, in the case of $^{12}\text{C}(p, \gamma_3)$, the expected interference structure would correspond to the fine levels of $\frac{7}{2}^-$ in ^{13}N .

IV. SUMMARY

Similar to the entrance channel configurations, the doorway states can be reached in radiative nucleon capture reactions either in a prompt way as the semidirect capture, or by a compound nucleus process. The former process stems from the part of the strength exhibiting giant resonances, while the latter arises from the part of the strength mixed into narrow levels. To investigate the interference effect between those two components in radiative capture reactions is the major objective of the present work.

Equation (14) presents a unified formalism to study radiative nucleon capture reactions, which includes the four nonstatistical mechanisms and their interference effects: namely, the potential capture, valence capture, semidirect capture, and fine resonance doorway capture.

The $^{12}\text{C}(p, \gamma_0)$ data at the excitation energy range from 10 to 30 MeV in ^{13}N were examined. Model calculations based upon the developed formalism were made to fit the measured data and extract the relevant model parameters. The results are presented in Fig. 1 and Tables I and II. Special attention was paid to investigate the interference between the $\frac{3}{2}^+$ fine levels and the $\frac{3}{2}^+$ giant resonances centered at $E_x = 13$ and 21 MeV. The valence widths for those levels were checked to be too small to account for the extracted widths, and the direct capture model proves unable to reproduce the background of the measured cross sections. It is shown that the observed dips at $E_x = 11.74$ and 14.04 MeV provide evidence of destructive interference in doorway states.

As an extension of the studies on $^{12}\text{C}(p, \gamma_0)$ and by examining the similarities of the final-state structure, we discuss the possibility of observing interferences of the doorway configurations in the reactions $^{12}\text{C}(n, \gamma_0)$ and $^{12}\text{C}(p, \gamma_3)$ [perhaps also $^{12}\text{C}(p, \gamma_1)$]. The reaction $^{12}\text{C}(n, \gamma_0)$ is expected to exhibit a similar interference structure as that of $^{12}\text{C}(p, \gamma_0)$, while $^{12}\text{C}(p, \gamma_3)$ shows interference between $\frac{7}{2}^-$ fine levels and broad resonances.

- [1] Y. K. Ho and M. A. Lone, Nucl. Phys. **A406**, 1 (1983); **A406**, 17 (1983).
- [2] Y. K. Ho, H. Kitazawa, and M. Igashira, Phys. Rev. C **44**, 1148 (1991).
- [3] S. Raman *et al.*, Phys. Rev. C **32**, 18 (1985), and references therein.
- [4] Y. K. Ho, J. F. Liu, and C. Coceva, *Nuclear Data Science Technology* (Mito, Japan, 1988), p. 703.
- [5] I. Bergqvist, in *Neutron Radiative Capture*, edited by R. E. Chrien (Pergamon, New York, 1988), p. 33, and references therein.
- [6] F. Ajzenberg-Selove, Nucl. Phys. **A360**, 1 (1981); **A449**, 1

- (1986); **A523**, 1 (1991), and references therein.
- [7] F. Ajzenberg-Selove, Nucl. Phys. **A281**, 69 (1977); **A375**, 72 (1982); **A480**, 1 (1986), and references therein.
- [8] Z. S. Yuan, Y. K. Ho, J. F. Liu, and Z. H. Lu, Phys. Rev. C **43**, 709 (1991).
- [9] D. F. Measday, M. Hasinoff, and D. J. Johnson, Can. J. Phys. **51**, 1227 (1973).
- [10] D. Berghofer, M. D. Hasinoff, R. Helmer, S. T. Lim, D. F. Measday, and K. Ebisawa, Nucl. Phys. **A263**, 109 (1976).
- [11] R. L. Helmer, M. D. Hasinoff, J. E. Bussoletti, K. A. Snover, and T. A. Trainor, Nucl. Phys. **A336**, 219 (1980).
- [12] K. A. Snover, P. G. Ikossi, E. G. Adelberger, and K. T.

- Lesko, Phys. Rev. Lett. **44**, 927 (1980).
- [13] P. Corvisiero, M. Aughinolfi, G. Ricco, M. Sauzone, M. Taiute, and A. Zucchiatti, Nucl. Phys. **A526**, 141 (1991).
- [14] M. Marangoni, P. L. Ottaviani, and A. M. Sasaruis, Nucl. Phys. **A277**, 239 (1977).
- [15] M. Micklinghoff, Nucl. Phys. **A295**, 237 (1978).
- [16] F. D. Becchetti and G. W. Greenless, Phys. Rev. **182**, 1190 (1969).
- [17] I. Bergqvist, D. M. Drake, D. K. Medaliels, S. A. Wender, A. Lindholm, L. Lilsson, N. Olsson, and R. Zorro, Nucl. Phys. **A456**, 426 (1986).
- [18] R. A. August, H. R. Weller, and D. R. Tolley, Phys. Rev. C **35**, 393 (1987).
- [19] A. Hakansson, A. Lindholm, L. Nilsson, J. Blomgren, P. O. Soderman, D. M. Drake, S. A. Wender, and N. Olsson, Phys. Rev. C **41**, 2556 (1990).
- [20] Z. D. Huang, L. H. Zhu, L. Ho, X. M. Shi, and D. Z. Ding, Chin. J. Nucl. Phys. **13**, 97 (1991).
- [21] J. W. Jury, B. L. Berman, D. D. Faul, P. Meyer, K. G. McNeill, and J. G. Woodworth, Phys. Rev. C **19**, 1684 (1979).
- [22] J. G. Woodworth, R. A. August, N. R. Roberson, D. R. Tilley, H. R. Weller, and J. W. Jury, Phys. Rev. C **29**, 1186 (1984).
- [23] S. Ferroni, G. Ricco, G. A. Rottigni, M. Sanzone, and G. Lo Bianco, IL Nuovo Cimento A **35**, 15 (1976).
- [24] S. L. Blatt, H. J. Hausman, L. G. Arnold, R. G. Seyler, R. N. Boyd, T. R. Donoghue, P. Konaz, M. A. Kovash, A. O. Bacher, and C. C. Foster, Nucl. Phys. **A30**, 423 (1984).
- [25] A. C. Shotter, S. Springham, D. Branford, J. Yorkston, J. C. McGeorge, B. Schoch, and P. Jennewein, Phys. Rev. C **37**, 1354 (1988).
- [26] S. V. Springham *et al.*, Nucl. Phys. **A517**, 93 (1990).
- [27] L. Van Hoorebeke *et al.*, Phys. Rev. C **42**, R1179 (1990).